
CALIBRATION AND TESTING OF A TERRESTRIAL LASER SCANNER

D. D. Lichti, M. P. Stewart, M. Tsakiri and A. J. Snow

School of Spatial Sciences
Curtin University of Technology
GPO Box U1987
Perth, WA 6845
AUSTRALIA
Phone: +61 8 9266 2691
Fax: +61 8 9266 2703
Email: lichti@vesta.curtin.edu.au

KEY WORDS: Laser scanning, calibration, deformation monitoring, target reduction.

ABSTRACT

Terrestrial laser imaging systems offer a new means for rapid precise mapping of objects up to ranges of up to a few hundred metres from the instrument location. The high sampling frequency (e.g., several kilohertz) available from such instrumentation can provide a spatial data density of directly observed co-ordinates far in excess of that available with photogrammetric techniques. For structural monitoring applications, this permits measurement of entire surfaces rather than a few discrete points, thus providing a wealth of information about the deformation modes of a body. This paper conveys the findings of a preliminary study of the resolution and accuracy of a commercially available laser-scanning system. Testing was conducted on a first order EDM calibration baseline and on a three-dimensional deformation-monitoring network. Single point range accuracies of $\pm 3\text{-}5$ cm (1σ) were achieved. Evidence of uncompensated systematic errors, probably due to instrumental set-up errors and target centre reduction, was detected.

1 INTRODUCTION

A terrestrial laser scanner is an active imaging device that can rapidly acquire a dense set of three-dimensional points on a large object or surface. Commercially available systems (at time of writing: February 2000) are capable of scan rates of up to 6 kHz at ranges of up to a few hundred metres. Such a high sampling frequency can produce data volumes on the order of several million points. Thus, this type of stand-alone instrumentation has great potential for close-range measurement tasks usually performed with photogrammetric methods. Such applications include slope stability and deformation monitoring, volume measurement for mining and civil engineering projects and as-built surveys. Perhaps the most significant benefit to monitoring applications is that a scanner can measure an entire surface with high resolution (literally millions of samples), whereas existing methods are limited to a few discrete points. Furthermore, as with airborne laser scanning systems, there is great potential for integration of laser scanner measurements with digital photogrammetric data.

In spite of the data rate and volume capabilities, the accuracy of commercially available scanners is, to the authors' knowledge, somewhat untested for such applications. Since manufacturers' specifications tend to vary from system to system, it would seem appropriate to quantify the performance of such instrumentation. Presented in this paper are the results from preliminary testing on the I-Site laser scanning system (<http://maptek.com.au/isite/>). The first testing stage was conducted on a first-order EDM baseline located at Curtin University of Technology. The second testing stage was performed on a high precision GPS-controlled rock fill dam monitoring network in Western Australia. The paper commences with a brief overview of laser scanning and a description of the testing. The data analysis procedure and results then follow. Finally, conclusions about the test results are presented along with recommendations on further research areas and applications for terrestrial laser scanning.

2 OVERVIEW OF TERRESTRIAL LASER SCANNING

2.1 Classes of Laser Scanners

Laser scanners may be categorised according to the means by which the range to an object is measured. While the physical principles of the different categories may vary, often they exhibit similarities in construction (e.g., oscillating mirrors and/or prisms). Some scanners operate on the principle of active triangulation, in which three-dimensional co-

ordinates are estimated from measurements of the incident and return beam directions (Beraldin *et al.*, 1993). Holographic scanners exploit the coherent nature of laser radiation to measure a surface by recording the interference pattern between two superimposed wave fronts (Vest, 1979). A pulsed laser scanner system, the subject of this study, derives range from measurement of the two-way flight time of a short laser pulse (Rueger, 1990). For greater detail about the principles of laser scanner operation, readers are referred to Marshall (1985), Baltasvias (1999b) and Wehr and Lohr (1999).

2.2 The I-Site Laser Scanner

The basic components of the I-Site system (pictured in Figure 1) are a pulsed diode laser, a return-signal detector and a beam deflection mechanism. The laser wavelength is $0.9\mu\text{m}$. As depicted in Figure 2, range measurements are derived from the return pulse time of flight measurement. The beam deflection mechanism complements the system to facilitate three-dimensional measurement. A rotating mirror allows a vertical field of view (FOV) of $\pm 40^\circ$, while the 300° horizontal FOV is provided by servomotor rotation. The scanner offers a 6 kHz data acquisition rate up to ranges of 350 m. A tribrach and level bubbles allow the instrument to be set up over an known survey monument, although these features were not available at the time of field testing (September 1999).



Figure 1. The I-Site scanner.

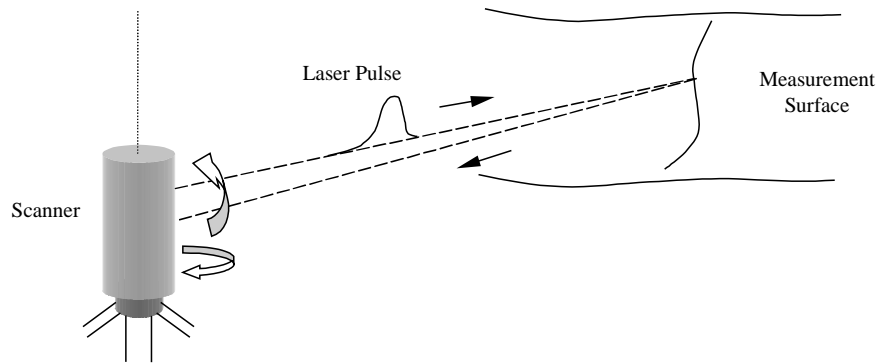


Figure 2. Terrestrial Laser Scanner Operation

3 TESTING

Two sets of tests were performed in order to evaluate the suitability of a terrestrial laser scanner for applications traditionally performed by photogrammetric means. The first test consisted of distance measurement comparison on the Curtin University EDM calibration baseline. The second test was conducted on a deformation-monitoring network situated on a rock fill dam in Western Australia.

3.1 EDM Baseline Testing

The EDM baseline at Curtin University is a series of twelve stable monuments spanning a total distance of approximately 600 metres. The scanner was positioned over one of the baseline pillars and targets were mounted on six others. Time constraints precluded measurement of all pillars. Set-up error was minimised by force centring and levelling both the instrument and targets. Each target consisted of a 10cm diameter, low-cost acrylic reflector affixed to a standard surveying target. The reflector constant for each target was predetermined. Temperature and pressure observations were recorded at each pillar at the time of each scan to permit correction due to atmospheric refraction.

3.2 Monitoring Network Testing

The North Dandalup dam south of Perth, Western Australia, has been monitored since 1996 using a combination of both conventional surveying and GPS positioning techniques. The main dam, illustrated in Figure 3, is of rock-fill construction, about 50 metres in height and inclined at an angle of approximately 60° . The previously described target assembly was installed at ten (of a total of 40) monitoring points on the dam complex. Each monitoring point was established by DGPS with an estimated accuracy of ± 5 mm in all three dimensions (Stewart *et al.*, 1999).

Scans were acquired from three locations around the main dam. Due to lack of force centring and levelling capabilities (since rectified), the position and orientation of the instrument remained unknown. Two scans were taken from each location, with the reflector assemblies oriented toward the instrument in each case. Figure 3 is a perspective projection of return signal strength from one of the scanner locations. The reflectors appear as the high intensity spots on the dam face.



Figure 3. North Dandalup Dam Scanner Image

3.3 Targeting for the Testing

The previously described target assemblies were used in each test to provide laser returns from specific points, thereby allowing easy recognition of the pillars and control points. However, such signalled targets are not required for scanning of general surfaces. Return signal strength is mainly a function of incidence angle, surface reflectivity and atmospheric conditions (Wehr and Lohr, 1999). The testing described herein relies upon the returns from the reflectors, which produce a response that is much stronger than that of the background materials (by up to a factor of four). In the subsequent analysis, it is therefore assumed that the accuracy of measured ranges to the reflective targets is independent of return signal strength.

4 DATA REDUCTION AND ANALYSIS

4.1 EDM Baseline Results

Due to the reflector size, beam divergence (approximately 3 mrad) and the fine measurement resolution (approximately 7' in elevation and direction), the target assemblies yielded multiple laser returns. This halo effect is schematically illustrated in Figure 4, in which there are several strong responses in the vicinity of the target. Spot size and brightness indicate return pulse strength as a function of position in the plane of the target assembly. The weaker responses result from peripheral beam returns having diminished power due to the Gaussian irradiance distribution, which decays as a function of beam radius (Marshall, 1985).

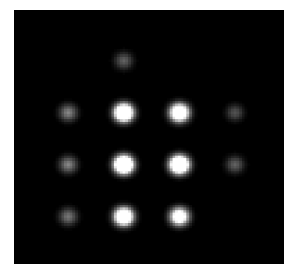


Figure 4. Halo Effect

The halo effect presents a problem of how to estimate the position of the target centre from a cluster of responses. Three approaches to perform this reduction were investigated:

1. The return position having maximum signal strength.
2. Radiometric centre of all n returns.
3. Radiometric centre of the 4 strongest returns.

In the case of 2 and 3 above, individual points were weighted by the intensity of their returns, i.e.:

$$\vec{V}_c = \frac{\sum_{i=1}^n E_i \vec{V}_i}{\sum_{i=1}^n E_i} \quad \text{for case 2, and} \quad \vec{V}_c = \frac{\sum_{i=1}^4 E_i \vec{V}_i}{\sum_{i=1}^4 E_i} \quad \text{for case 3,} \quad (1)$$

where

- \vec{V}_c is the three-dimensional radiometric centre of the target,
- \vec{V}_i is the position vector (x,y,z) of scanned point “i”, and
- E_i is the quantized energy of the return signal from scanned point “i”.

This intensity-based weighting strategy implicitly assumes that the strongest signal should be returned from the centre of the reflective target. Non-orthogonality of the incident beam relative to the reflector and the uniform sampling strategy of the scanner violate this assumption. Therefore, any reduction technique involving prism reflectors may introduce an error source in addition to those associated with instrumental noise, location of the electrical centre of the instrument, and the transmission of the signal through the atmosphere.

Presented in Figure 5 are the residual differences between the known baseline horizontal distances to each pillar and the derived distances from each scan, for each of the three previously mentioned reduction techniques. The mean residual offsets and associated standard deviations for each technique are $0.018 \pm 0.029\text{m}$, $0.039 \pm 0.048\text{m}$ and $0.0279 \pm 0.037\text{m}$, respectively. Given the sample size (a total number of 18 scans), there would appear to be a small bias suggesting that the measurements from the laser scanner are systematically shorter than the true baseline lengths. This could be due to uncertainty about the location of the instrument’s electrical centre. From this data set, there appears to be no increase in the scatter of errors as baseline length increases, indicating the system is functioning without serious distance-dependent bias up to distances of 260m.

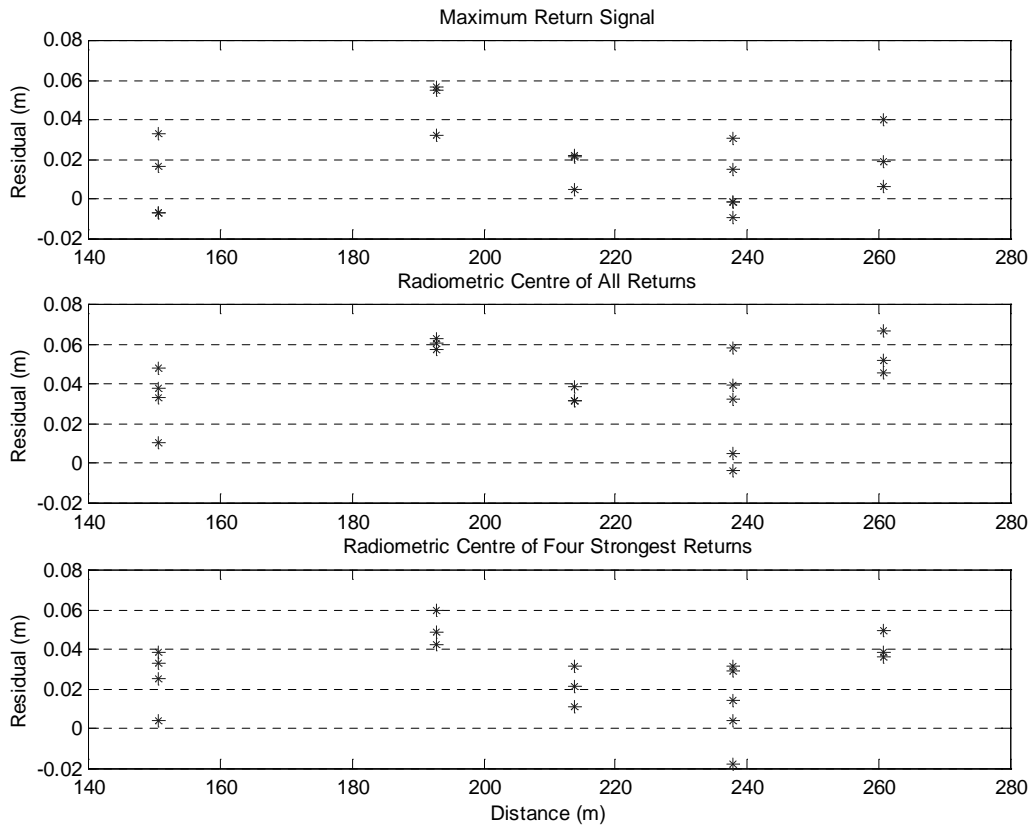


Figure 5. Calibration Baseline Residuals for each Reduction Method.

Table 1 summarises individual baseline component repeatability for each reduction strategy for pillar 7 (4 repeat scans) and pillar 11 (5 repeat scans), these pillars offering a larger sample of repeat scans than others. The x- and y-axes of the scanner were nominally parallel and orthogonal to the baseline, respectively. Here, some differences between analysis techniques are evident. Although the horizontal distance standard errors are fairly consistent at the 15 – 25mm level for both pillars, vector components show markedly more variability (note the z or height component was not used in the horizontal distance computation). Reduction method 1 (maximum return only) produces a repeatability of greater than 10cm for pillar 7 and 20cm in y for pillar 11. As might be expected, reduction method 3 (4 strongest returns) does not differ much from method 2, but does show variability up to nearly 13cm on the y component of pillar 11.

It would appear that a certain degree of randomness is present in the reduction of a series of point laser returns from a reflective prism to an individual known control point. The angle of incidence of the beam on the prism and the location of each incident beam can produce variable results. These are more a function of the reduction processes involved in attempting to apply control to the laser scanner data than the actual accuracy of a single measurement from the scanner, *per se*. From Table 1, reduction method 2 (radiometric centre) generally exhibits the least variability and therefore was adopted for analysis of the North Dandalup Dam data.

Pillar 7		4 Repeat Scans		Calibrated Distance: 150.674 m	
Reduction method	σ_x (m)	σ_y (m)	σ_z (m)	σ in horizontal distance (m)	
1	± 0.022	± 0.104	± 0.024	± 0.019	
2	± 0.020	± 0.056	± 0.015	± 0.016	
3	± 0.018	± 0.042	± 0.041	± 0.015	

Pillar 11		5 Repeat Scans		Calibrated Distance: 237.711 m	
Reduction method	σ_x (m)	σ_y (m)	σ_z (m)	σ in horizontal distance (m)	
1	± 0.038	± 0.203	± 0.000	± 0.016	
2	± 0.026	± 0.060	± 0.095	± 0.025	
3	± 0.029	± 0.127	± 0.088	± 0.020	

Table 1. Results from Repeat Scans on the EDM Calibration Baseline.

It may be inferred that the horizontal distance repeatabilities and the comparison of horizontal distances with the truth from the EDM calibration baseline represent an indication of the true accuracy of individual scanned points. Although horizontal distances are derived from a number of point samples, these are distributed more in the vertical plane than the horizontal due to reflector orientation. Therefore, reduction processes will affect horizontal range measurements less than the individual vector components, so long as the height difference between the instrument and target is small, as on the baseline.

4.2 Monitoring Network Results

At the time of the test (September 1999), it was not possible to centre the I-SiTE unit on a tripod over a known point due to the lack of level bubbles and forced centring. Also, some doubt existed regarding the exact location of the electrical centre of the unit, particularly given the results from the calibration baseline described above. Therefore, for each of the 6 scans at North Dandalup, the phase centre and three orientation angles of the scanner were estimated via three-dimensional resection from the ten known control points on the dam wall.

The geometry of the three-dimensional resection is depicted in Figure 6. Here, the scanner is positioned at S with arbitrary orientation relative to object space, and point P is being imaged. Since the scanner observables are co-ordinates, the resection problem can be formulated as a three-dimensional rigid body transformation of points from object space to scanner space. The resection equation for point “p” is given by

$$\begin{pmatrix} x \\ y \\ z \end{pmatrix}_p = M(\omega, \phi, \kappa) \begin{pmatrix} X_p - X_s \\ Y_p - Y_s \\ Z_p - Z_s \end{pmatrix} \quad (2)$$

where

$$\begin{pmatrix} x & y & z \end{pmatrix}_p^T \quad \text{are the observed co-ordinates of point “p” in scanner space (vector SP in Figure 6),}$$

$$\begin{pmatrix} X & Y & Z \end{pmatrix}_p^T \quad \text{are the object space co-ordinates of point “p” (vector OP),}$$

$$(X \ Y \ Z)_s^T$$

are the object space co-ordinates of the scanner space origin (electrical centre of the instrument; vector OS), and

$$M(\omega, \phi, \kappa)$$

is the rotation matrix from object space to scanner space, parameterised in terms of the Cardan angles ω , ϕ and κ .

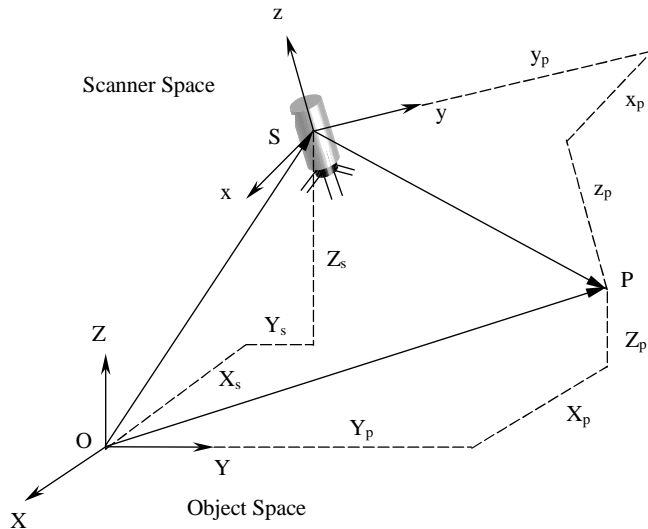


Figure 6. Laser Scanner Resection Geometry.

yields a ‘measurement repeatability’ independent of both the GPS co-ordinates, and the supposed position of the electrical centre of the I-SiTE instrument. Unlike the results presented above for pillars 7 and 11, only two repeat scans are available for each scanner location and each point on North Dandalup. However, a total of 28 repeats are available. Co-ordinate differences between the two scans are shown in Figure 8. The repeatabilities are $-0.010 \pm 0.066\text{m}$, $-0.014 \pm 0.038\text{m}$ and $0.021 \pm 0.037\text{m}$ in the x , y and z components, respectively. Once again, no distance dependence is obvious. However, it is interesting to note that the points located at the furthest ranges (at 247m and 257m) exhibit the largest overall repeatabilities (in terms of difference vector magnitude) of 0.281m and 0.169m, respectively. It can also be seen from Figure 8 that, in general, scans at distances under 100m have lower repeatabilities in all components. However, given the size of the data sample, these observations are not conclusive. Similar analysis of repeatability against direction to the control point from the scanner yielded no apparent correlation; i.e., results appear to be independent of direction as well as distance from the instrument. However, only about one third of the scanner’s horizontal angular range was utilised.

4.3 Discussion

The initial aim of the tests described in this paper was to assess the accuracy and resolution of an optical laser scanner over distances of up to 250m. However, the strategy of placing reflective prisms at known points to provide control for the vector measurements is hindered by the nature of the scanning apparatus itself. A user has no control over beam alignment (i.e., one cannot point to a particular point) due to the scanner’s uniform sampling scheme (in both elevation and direction). This issue is perhaps not such a problem given the large number of points to be collected, but does pose some issues for benchmark calibration tests.

All results are contaminated by the technique of reducing a number of vector co-ordinates from a cluster of returns to a single central point that is assumed to be coincident with the known control point. Only the ‘maximum return’ method (method 1 in Section 4 above) is immune to this problem. However, it has been demonstrated that the maximum return from the prism is not necessarily coincident with the centre of the prism and cannot be reduced to the known control point without error. Intuitively, the accuracy of individual point vectors may be more optimistic than the above results indicate.

The best indication of the accuracy of the instrument would appear to come from the horizontal distances measured on the calibration baseline. Here, the distribution of points in the vertical plane of the reflector has least influence on the horizontal range. This is not the case at North Dandalup Dam where height differences of up to 50m existed between the reflector and the scanner location. In these cases, the angle of incidence of the laser pulse on the reflectors would be far from normal. The horizontal repeatabilities from Table 1 of $\pm 1.5 - 2.5\text{cm}$ probably represent the ‘cleanest’ estimate

Results from the resection are shown in Figure 7, in which the estimated residuals in each dimension have been plotted as a function of range. The standard deviations of the 58 residuals (for each dimension) are: $\pm 0.043\text{m}$ in x , $\pm 0.023\text{m}$ in y and $\pm 0.034\text{m}$ in z . The maximum residual is -0.125m . These standard deviations include the uncertainty in the GPS co-ordinates but, by solving for its location, exclude the uncertainty in the position of the electrical centre of the scanner. As with the EDM calibration baseline test, no dependence on baseline length is evident from the x , y , z component graphs.

Direct comparison of the repeat measurements of three dimensional vector to the reduced centre of each control point

of scanner accuracy, although a bias does appear to exist in the baseline length when the horizontal distances are compared with the truth. Results from North Dandalup indicate an accuracy of approximately $\pm 3 - 7$ cm, with some large repeatabilities on individual baseline components. Again, these represent more a deficiency in the data reduction techniques than the true resolution of the scanner.

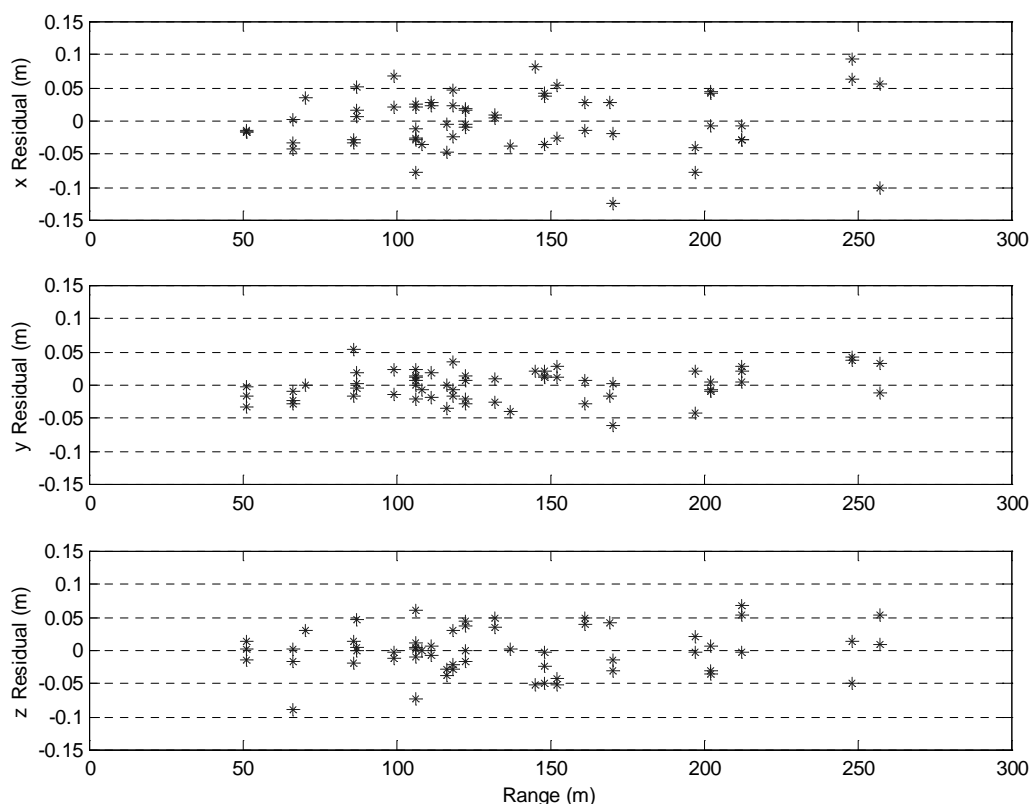


Figure 7. Monitoring Network Resection Residuals from all Six Scans.

5 CONCLUSIONS AND RECOMMENDATIONS

Terrestrial laser scanning technology offers surveyors and photogrammetrists a rapid means of collecting dense sets of three-dimensional point sets. For structural monitoring applications, laser scanning can be considered advantageous over geodetic methods (e.g., surveying, GPS), which can only sense deformation at a limited number of points, whereas a scanner can measure a deformation *surface*. Furthermore, unlike photogrammetric techniques, scanning provides direct co-ordinate measurement and does not rely upon matching strategies to solve the correspondence problem between conjugate feature points within the scene (Baltsavias, 1999a).

Preliminary benchmark testing of one scanner has been conducted, from which the best estimate of range accuracy was $\pm 3 - 5$ cm, with repeatability at the level of $\pm 1.5 - 2.5$ cm. Several important issues about this type of instrumentation have been raised, however. A bias was apparent from the EDM calibration baseline tests, which may be directionally dependent (i.e., due to eccentricity). This requires further investigation.

Reflective targets were used to perform the benchmark testing. Due to sampling, beam divergence and reflector size, scans of these targets suffered from a halo effect (multiple laser responses). While three target reduction methods were investigated, no single method clearly outperformed the others, although the radiometric centre method would seem to be the most logical choice. Further testing is required to improve the reduction technique and/or the choice of target.

As previously mentioned, the high sample point density provided by terrestrial laser scanner technology offers a wealth of information for structural monitoring applications. Such dense data sets give rise to issues such as data handling, filtering and suitable deformation analysis procedures. Future work will concentrate on these aspects as well as integration of laser scanner data with measurements from other sensors (e.g., GPS, digital cameras).

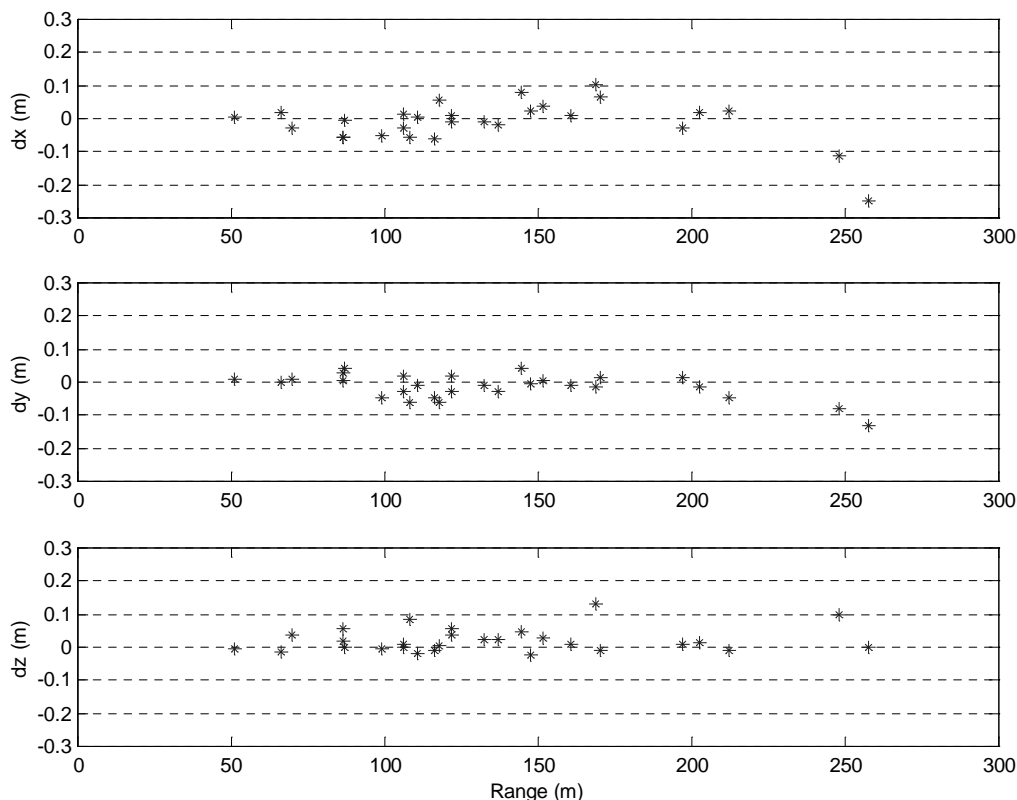


Figure 8. Monitoring Network Co-ordinate Differences from all 28 Points.

ACKNOWLEDGMENTS

The authors gratefully acknowledge the support of Maptek Pty. Ltd., Whelans Surveys and Mapping Pty. Ltd. and Leica Geosystems Pty. Ltd. (Western Australia).

REFERENCES

- Baltsavias, E. P., 1999a. A comparison between photogrammetry and laser scanning. *ISPRS Journal of Photogrammetry and Remote Sensing*, 54 (2-3): 83-94.
- Baltsavias, E. P., 1999b. Airborne laser scanning: basic relations and formulas. *ISPRS Journal of Photogrammetry and Remote Sensing*, 54 (2-3): 199-214.
- Beraldin, J. -A., S. F. El-Hakim and L. Cournoyer, 1993. Practical range camera calibration. In *Videometrics 2*, SPIE vol. 2067, Boston, USA, pp. 21-31.
- Marshall, G. F. (Ed.), 1985. *Laser Beam Scanning: Opto-Mechanical Devices, Systems and Data Storage Optics*. New York: Macel Dekker, Inc.
- Rueger, J. M., 1990. *Electronic Distance Measurement*. Berlin: Springer-Verlag.
- Stewart, M. P., M. Tsakiri and R. Duckrell, 1999. Dam deformation monitoring with episodic GPS. In *Proceedings of the Sixth South East Asian Surveyors Congress*, Fremantle, WA, pp. 477-484.
- Vest, C. M., 1979. *Holographic Interferometry*. New York: John Wiley & Sons.
- Wehr, A. and U. Lohr, 1999. Airborne laser scanning – an introduction and overview. *ISPRS Journal of Photogrammetry and Remote Sensing*, 54 (2-3): 68-82.